

Turbulent Flow in Pipes and Channels as Cross-Stream “Inverse Cascades” of Vorticity

Gregory L. Eyink

Applied Mathematics & Statistics, The Johns Hopkins University, Baltimore, MD 21218

Center for Nonlinear Studies, Los Alamos National Laboratory, Los Alamos, NM 87545

Abstract

A commonplace view of pressure-driven turbulence in pipes and channels is as “cascades” of streamwise momentum toward the viscous layer at the wall. We present in this paper an alternative picture of these flows as “inverse cascades” of spanwise vorticity, in the cross-stream direction but away from the viscous sublayer. We show that there is a constant spatial flux of spanwise vorticity, due to vorticity conservation, and that this flux is necessary to produce pressure-drop and energy dissipation. The vorticity transport is shown to be dominated by viscous diffusion at distances closer to the wall than the peak Reynolds stress, well into the classical log-layer. The Perry-Chong model based on “representative” hairpin/horsehoe vortices predicts a single sign of the turbulent vorticity flux over the whole log-layer, whereas the actual flux must change sign at the location of the Reynolds-stress maximum. Sign-reversal may be achieved by assuming a slow power-law decay of the Townsend “eddy intensity function” for wall-normal distances greater than the hairpin length-scale. The vortex-cascade picture presented here has a close analogue in the theory of quantum superfluids and superconductors, the “phase slippage” of quantized vortex lines. Most of our results should therefore apply as well to superfluid turbulence in pipes and channels. We also discuss issues about drag-reduction from this perspective.

1 Introduction

It is quite standard to view turbulence in pipes, channels and ducts, as well as other wall-bounded turbulent boundary layers, as spatial “cascades” of momentum in the wall-normal or cross-stream direction. For example, we may quote from a well-known monograph [1]:

“There exists a close analogy between the spatial structure of turbulent boundary layers and the spectral structure of turbulence. At sufficiently large Reynolds numbers, the overall dynamics of turbulent boundary layers is independent of viscosity just as the large-scale spectral dynamics of turbulence is. In the wall layer of a turbulent boundary layer, viscosity generates a ‘sink’ for momentum, much like the dissipative sink for kinetic energy at the small-scale end of the turbulence spectrum. In particular, the asymptotic rules governing the link between the large-scale description and the small-scale description lead to the closely related concepts of an inertial subrange in the turbulence energy spectrum...and an inertial sublayer in wall-bounded shear flows.”

— Tennekes & Lumley (1972)

In this point of view, the logarithmic mean velocity profile is analogous to the Kolmogorov $-5/3$ power-law energy spectrum, and the constant Reynolds stress through the inertial sublayer is analogous to the constant energy flux through the inertial subrange. As expressed in the quote above, high momentum from the outer region of the boundary layer is transported inward by the constant Reynolds stress and ultimately transferred to the wall by viscous stress.

There is, however, another complementary process in wall-bounded turbulence of at least equal importance. Vorticity generated at the wall is transported outward, diffused first by viscosity and subsequently advected by turbulent velocity fluctuations. Due to the fundamental hydrodynamic principle of vorticity conservation [2, 3], the wall-normal flux of spanwise vorticity is constant over the whole cross-section of the flow. The “sink” of vorticity at the outer range is provided by cancellation with vorticity of the reverse sign transported from the wall on the opposite side of the flow. There is thus a spatial “inverse cascade” of vorticity co-existing with

the “forward cascade” of momentum. Furthermore, it may be shown that the constant flux of spanwise vorticity in this “inverse cascade” is crucially related to the energy dissipation and wall drag in turbulent pipe and channel flows. This relation was first observed in early work of Taylor [4], but seems not to have been as widely appreciated as it deserves in the fluid dynamics community. Although there have been very many studies of the Reynolds stress—or turbulent momentum transport—in pipe and channel flow, there have been far fewer investigations of the turbulent vorticity-transport tensor in classical fluid turbulence. Notable exceptions are the experimental works by Klewicki and collaborators [5, 6, 7, 8] and a theoretical and DNS study of Bernard [9]. In the meantime, Taylor’s observation of the relation between cross-stream transport of vorticity and downstream pressure drop has been rediscovered in the field of quantum superfluids, where it goes by the name of the “Josephson-Anderson relation” [10, 11]. The cross-stream motion or phase slippage of quantized vortex lines is widely recognized to be a key mechanism of energy dissipation in quantum superfluids and superconductors [12, 13].

The purpose of this paper is to expound in detail the picture of pipe and channel flows, or other pressure-driven turbulent flows, as spatial “inverse cascades” of vorticity co-existing with the more commonly recognized “forward cascade” of momentum. Although several of the results presented here are to be found in the existing literature, there seems to be no systematic presentation of this fundamental point of view of wall-bounded turbulence. It is hoped that the discussion here will help to stimulate some further experimental and numerical efforts to elucidate the relevant vortex dynamics in turbulent flows. In addition, this paper will discuss the close analogy between vortex dynamics in classical turbulence and in quantum superfluids. A very interesting paper on this subject has been written by Huggins [14], from the vantage of the low-temperature physicist. We shall further elaborate upon his discussion, filling in some of the details on classical fluid turbulence. Needless to say, comparisons between such disparate areas of physics can often be extremely illuminating and can stimulate new questions and different points of view in both subjects.

2 Vorticity Conservation and Generation at the Boundary

We begin by briefly reviewing some basic results on vorticity in classical fluid dynamics, its associated conservation law and its generation at solid walls. This is necessary in order to set the stage for our following discussion on wall-bounded turbulence. Furthermore, even this very classical subject is not without controversy, as there is currently some disagreement about the proper form of the vorticity source at the wall [15, 17].

2.1 The Helmholtz Equation as Conservation Law

The evolution of vorticity in classical incompressible fluids is described by the equation of Helmholtz [2]

$$\partial_t \boldsymbol{\omega} + (\mathbf{u} \cdot \nabla) \boldsymbol{\omega} = (\boldsymbol{\omega} \cdot \nabla) \mathbf{u} + \nu \Delta \boldsymbol{\omega} + \nabla \times \mathbf{f}, \quad (1)$$

supplemented by terms representing viscous diffusion with kinematic viscosity ν and the curl of a non-potential body force \mathbf{f} (e.g. from electromagnetic stirring [21] or stress from polymer additives [22, 23]). Because this equation is obtained by taking the curl of the momentum equation, or incompressible Navier-Stokes equation, it must take the form of a local conservation law. Explicitly, (1) can be rewritten as [14]

$$\partial_t \boldsymbol{\omega} + \nabla \cdot \boldsymbol{\Sigma} = \mathbf{0} \quad (2)$$

or $\partial_t \omega_j + \partial_i \Sigma_{ij} = 0$, where

$$\Sigma_{ij} = u_i \omega_j - u_j \omega_i + \nu \left(\frac{\partial \omega_i}{\partial x_j} - \frac{\partial \omega_j}{\partial x_i} \right) + \epsilon_{ijk} f_k. \quad (3)$$

This anti-symmetric tensor represents spatial flux of the j th component of vorticity in the i th coordinate direction. It plays a fundamental role in all of our following considerations. The first term on the righthand side of (3) represents convective transport, while the second term represents spatial transport by vortex-shearing, the third term describes viscous diffusion and the fourth term gives the induced motion of vorticity due to Magnus effect of the body force.

Because vorticity arises as the curl of the velocity, $\boldsymbol{\omega} = \nabla \times \mathbf{u}$, the above conservation law must be in some sense “trivial”. This is the content of Föppl’s Theorem [3], which states that the total vorticity integrated over the flow domain Ω must vanish: $\int_{\Omega} \boldsymbol{\omega} d^3x = \mathbf{0}$. This result holds in an infinite domain with sufficiently rapidly decaying vorticity at infinity, or in a bounded domain with uniformly moving, solid walls (but not, for example, in a rotating container). The standard proof is based on the simple identity $\boldsymbol{\omega} = \nabla \cdot (\boldsymbol{\omega} \mathbf{x})$, which implies by the divergence theorem that $\int_{\Omega} \boldsymbol{\omega} d^3x = \int_{\partial\Omega} \mathbf{x}(\boldsymbol{\omega} \cdot \hat{\mathbf{n}}) dA$ for the outward-pointing normal $\hat{\mathbf{n}}$ on the bounding surface $\partial\Omega$. On a solid wall in uniform motion, $\boldsymbol{\omega} \cdot \hat{\mathbf{n}} = 0$, because of stick boundary conditions for the velocity field. There is also no contribution from boundary points at infinity, if $|\boldsymbol{\omega}| = o(|\mathbf{x}|^{-3})$ as $|\mathbf{x}| \rightarrow \infty$. This result shows that complete cancellation of vorticity must occur when integrated over the entire domain of such flows, despite strong localized vortex structures of various orientations distributed throughout the fluid.

2.2 Lighthill’s Theory of Vorticity Generation at Solid Walls

If the vorticity conservation law (2) is integrated over the flow domain, one obtains

$$\frac{d}{dt} \int_{\Omega} \boldsymbol{\omega} d^3x = \int_{\partial\Omega} \boldsymbol{\Sigma} \hat{\mathbf{n}} dA. \quad (4)$$

Of course, under the conditions of Föppl’s Theorem, which we hereafter assume, $\int_{\partial\Omega} \boldsymbol{\Sigma} \hat{\mathbf{n}} dA = \mathbf{0}$. As argued by Lyman [15], the relation (4) motivates one to consider $\boldsymbol{\sigma} = \boldsymbol{\Sigma} \hat{\mathbf{n}}$ as a source density for vorticity at the wall, with strength $|\boldsymbol{\sigma}|$ in the direction $\hat{\boldsymbol{\sigma}} = \boldsymbol{\sigma}/|\boldsymbol{\sigma}|$. As a consequence of anti-symmetry of $\boldsymbol{\Sigma}$, the vortex lines generated are parallel to the surface, since $\boldsymbol{\sigma} \cdot \hat{\mathbf{n}} = 0$ [16]. However, Wu and Wu [17] have pointed out that such a global argument is insufficient to identify $\boldsymbol{\sigma}$ as a local source of vorticity, since it may be altered by adding any perturbation $\delta\boldsymbol{\sigma}$ such that $\int_{\partial\Omega} \delta\boldsymbol{\sigma} dA = \mathbf{0}$. In the Appendix A, we present a proof based upon the Kelvin Theorem which shows that $\boldsymbol{\sigma} = \boldsymbol{\Sigma} \hat{\mathbf{n}}$ does represent a localized source of vorticity at the boundary. This holds in the following precise sense: If one considers *any* loop C in the fluid with part of its length lying in the boundary $\partial\Omega$, then the contribution of the boundary segment to the time-derivative of

the vorticity flux through C is given by

$$\int_{C \cap \partial\Omega} \boldsymbol{\sigma} \cdot (\hat{\mathbf{n}} \times \hat{\mathbf{t}}) ds$$

where $\hat{\mathbf{t}}$ is the unit tangent vector along the curve C , for a specified orientation. With this convention the flux is measured positive in the direction to the righthand side of the curve C as one moves along it, i.e. parallel to $\hat{\mathbf{n}} \times \hat{\mathbf{t}}$.

Using the expression (3) for $\boldsymbol{\Sigma}$, it follows that

$$\boldsymbol{\sigma} = -\hat{\mathbf{n}} \times \nu (\nabla \times \boldsymbol{\omega}) + \hat{\mathbf{n}} \times \mathbf{f} \quad (5)$$

due to the no-through condition $\mathbf{u} \cdot \hat{\mathbf{n}} = 0$ for an impermeable wall and the result $\boldsymbol{\omega} \cdot \hat{\mathbf{n}} = 0$ for a solid wall in uniform motion. Further insight and simplification can be obtained if one uses the Navier-Stokes momentum balance $D_t \mathbf{u} = -\nabla p - \nu \nabla \times \boldsymbol{\omega} + \mathbf{f}$ to give [18]

$$\boldsymbol{\sigma} = \hat{\mathbf{n}} \times (\nabla p + D_t \mathbf{u}).$$

This form of the vorticity source density was first derived by Lighthill [24] and Morton [25] who obtained the terms from the tangential pressure gradient and the tangential boundary acceleration, respectively. The term identified by Morton, $\hat{\mathbf{n}} \times (D_t \mathbf{u})$, contributes only if the boundary is accelerating continuously or impulsively. If we restrict our attention to constant-velocity (or stationary) boundaries, then we recover the original Lighthill (1963) result

$$\boldsymbol{\sigma} = \hat{\mathbf{n}} \times (\nabla p). \quad (6)$$

This formula has several remarkable implications [25]. First, one can see that the generation of vorticity is essentially *inviscid*. Second, the generated vortex lines on boundary $\partial\Omega$ are parallel to the surface isobars, or lines of constant pressure p .

2.3 Mean Flux of Vorticity in Pressure-Driven Flows

In turbulent flow, the vorticity balance (2) may be considered in Reynolds-averaged form:

$$\partial_t \bar{\boldsymbol{\omega}} + \nabla \cdot \bar{\boldsymbol{\Sigma}} = \mathbf{0} \quad (7)$$

where the mean vorticity flux tensor is

$$\bar{\Sigma}_{ij} = \bar{u}_i \bar{\omega}_j - \bar{u}_j \bar{\omega}_i + \overline{u'_i \omega'_j - u'_j \omega'_i} + \nu \left(\frac{\partial \bar{\omega}_i}{\partial x_j} - \frac{\partial \bar{\omega}_j}{\partial x_i} \right) + \epsilon_{ijk} \bar{f}_k. \quad (8)$$

The first term $\bar{u}_i \bar{\omega}_j - \bar{u}_j \bar{\omega}_i$ represents the transport of mean vorticity by the mean flow. On the other hand, the term $\overline{u'_i \omega'_j - u'_j \omega'_i}$ represents the transport of mean vorticity by the fluctuations and is the analogue of the Reynolds stress in the ensemble-averaged momentum balance.

We now derive a crucial relationship between mean vorticity transport and mean pressure gradients. The Navier-Stokes equation may be written as $\partial_t u_k = \frac{1}{2} \epsilon_{klm} \Sigma_{lm} - \partial_k (p + U + \frac{1}{2} |\mathbf{u}|^2)$ in terms of Σ and the potential U of any conservative body force (e.g. gravity). In statistically stationary turbulence, the time-derivative averages to zero, so that one obtains

$$\overline{\partial_k (p + U + \frac{1}{2} |\mathbf{u}|^2)} = \frac{1}{2} \epsilon_{klm} \bar{\Sigma}_{lm}, \quad \bar{\Sigma}_{ij} = \epsilon_{ijk} \overline{\partial_k (p + U + \frac{1}{2} |\mathbf{u}|^2)}. \quad (9)$$

To our knowledge, this relation was first derived by Taylor [4] for a general turbulent shear-flow, assuming strict two-dimensionality of the fluctuations. His work is discussed in Section 3 below, on turbulence in pipes and channels. More than thirty years later, this result was rediscovered by Anderson [10], who considered inviscid flow with no body forces. His work will be considered in Section 4 on quantum superfluids. The full relationship (9) was derived by Huggins [14], as a ‘‘Josephson-Anderson relation’’ for classical turbulence.

Another useful form of this relation can be derived by using the standard vector-calculus identity $(\bar{\mathbf{u}} \cdot \nabla) \bar{\mathbf{u}} = \bar{\mathbf{u}} \times \bar{\boldsymbol{\omega}} - \nabla \cdot (\frac{1}{2} |\bar{\mathbf{u}}|^2)$ to write the Reynolds-averaged Navier-Stokes equation as

$$\bar{D}_t \bar{u}_k = \frac{1}{2} \epsilon_{klm} \bar{\Sigma}_{lm}^* - \partial_k \bar{p}^*,$$

with

$$\bar{\Sigma}_{ij}^* = \overline{u'_i \omega'_j - u'_j \omega'_i} + \nu \left(\frac{\partial \bar{\omega}_i}{\partial x_j} - \frac{\partial \bar{\omega}_j}{\partial x_i} \right) + \epsilon_{ijk} \bar{f}_k \quad (10)$$

and $\bar{p}^* = \bar{p} + U + k$, where $k = \frac{1}{2} \overline{|\mathbf{u}'|^2}$ is the turbulent kinetic energy and $\bar{D}_t = \partial_t + \bar{\mathbf{u}} \cdot \nabla$ is the material time-derivative for the mean flow. Thus, in cases where $\bar{D}_t \bar{\mathbf{u}} = \mathbf{0}$,

$$\partial_k \bar{p}^* = \frac{1}{2} \epsilon_{klm} \bar{\Sigma}_{lm}^*, \quad \bar{\Sigma}_{ij}^* = \epsilon_{ijk} \partial_k \bar{p}^*. \quad (11)$$

In this version of the relationship, the vorticity transport by the mean flow is omitted and gradients in the “turbulent enthalpy” $\bar{p}^* = \bar{p} + U + k$ are considered.

We now consider the implications of these results for turbulent channel and pipe flows.

3 Channel and Pipe Flows

As usual, channel flow refers to fluid motion between two parallel, infinite plane walls separated by distance $2h$, with a pressure gradient parallel to the planes. Our notations follow those of [1]. Thus, we take x to be the streamwise direction (along the pressure gradient), z the spanwise direction, and y the wall-normal or cross-stream direction, with $y = 0$ at the bottom plate. The velocity field is then represented as $\mathbf{u} = (u, v, w)$ in terms of its streamwise, wall-normal, and spanwise components. It is assumed that the turbulence is fully developed, in the sense that it is statistically stationary and that all averages are independent of z and also (except for the mean pressure \bar{p}) independent of x . The only non-vanishing component of mean velocity is $\bar{u}(y)$, with a maximum value $\bar{u}_c = \bar{u}(h)$ at the channel centerplane. The mean vorticity has only a spanwise component, $\bar{\omega}_z(y) = -\partial\bar{u}/\partial y$, which is negative for $y < h$ and positive for $y > h$.

Pipe flow refers instead to fluid motion down an infinitely long, cylindrical pipe with circular cross section of radius ρ , driven by a pressure gradient down the pipe axis. We use standard cylindrical coordinates (r, θ, z) , so that z represents the streamwise/axial direction, θ the azimuthal direction, and r the radial/wall-normal/cross-stream direction. We write the velocity as $\mathbf{u} = (u_r, u_\theta, u_z)$ and similarly for other vector quantities. In fully developed pipe turbulence, all average quantities are independent of t, θ and z , except that mean pressure \bar{p} decreases linearly with z . The only non-vanishing component of mean velocity is $\bar{u}_z(r)$, with a maximum value $\bar{u}_c = \bar{u}_z(0)$ at the center axis. The mean vorticity has only an azimuthal component, $\bar{\omega}_\theta(r) = -\partial\bar{u}_z/\partial r > 0$. Because these two problems are so similar, we shall give full details only for channel flow and then comment upon the relevant differences for pipe flow.

3.1 Mean Vorticity Flux and Energy Dissipation

In channel flow, the relations (11) become

$$\overline{v'\omega'_z - w'\omega'_y} - \nu \frac{\partial \bar{\omega}_z}{\partial y} = \bar{\Sigma}_{yz}^* = \frac{\partial \bar{p}^*}{\partial x} \quad (12)$$

$$\overline{w'\omega'_x - u'\omega'_z} = \bar{\Sigma}_{zx}^* = \frac{\partial \bar{p}^*}{\partial y} \quad (13)$$

$$\overline{u'\omega'_y - v'\omega'_x} = \bar{\Sigma}_{xy}^* = 0. \quad (14)$$

Note that $\bar{\Sigma}_{ij} = \bar{\Sigma}_{ij}^*$ for all i, j except $\bar{\Sigma}_{zx} = -\bar{\Sigma}_{xz} = -\bar{u}\bar{\omega}_z + \bar{\Sigma}_{zx}^*$. As should be clear from the general derivation, these relations are just the usual momentum balance equations written in a different form. For example, it is easy to check that

$$\overline{v'\omega'_z - w'\omega'_y} = -\frac{\partial}{\partial y} \overline{u'v'}, \quad -\nu \frac{\partial \bar{\omega}_z}{\partial y} = \nu \frac{\partial^2 \bar{u}}{\partial y^2} \quad (15)$$

See also [1], eq.(3.3.13), or [5]. However, now (12)-(14) are seen to have another, equally important interpretation: they relate the pressure gradients in various directions to the corresponding cross-fluxes of a transverse component of vorticity. The first relation (12) was already derived by Taylor [4] in a slightly modified form for two-dimensional flow, as mentioned earlier. Taylor employed this relation, which is exact, to motivate his well-known “vorticity transfer hypothesis,” which assumes gradient-transport of vorticity. As discussed in [1], section 3.3, the latter hypothesis ignores vortex-stretching interactions and has limited validity (but see [9] for a refinement). As a consequence, this paper of Taylor’s has fallen into a bit of disrepute and it is not usually noted that a significant exact result was derived there.

Of the relations (12)-(14), the most important is indeed (12), since it relates the cross-stream flow of spanwise vorticity $\bar{\Sigma}_{yz}$ to the streamwise pressure gradient $\partial \bar{p} / \partial x$. Note that $\partial \bar{p}^* / \partial x = \partial \bar{p} / \partial x$, since U is zero and k is independent of x . It is well-known that the mean streamwise pressure-gradient is constant across a cross-section of the channel, i.e. $\partial \bar{p} / \partial x = -\gamma_*$ independent of y . However, in standard derivations (e.g. [1], section 5.2) this appears to be an “accident”. Here it is seen that the fundamental reason is the conservation of vorticity:

$$\frac{\partial}{\partial y} \left(\frac{\partial \bar{p}}{\partial x} \right) = \partial_y \bar{\Sigma}_{yz} = 0.$$

It is easy to determine its constant value by the balance of stress at the two walls against the pressure-gradient applied over a channel cross-section, giving $-2u_*^2 = (2h)\frac{\partial\bar{p}}{\partial x}$, or $\frac{\partial\bar{p}}{\partial x} = -\gamma_* = -u_*^2/h$ in terms of the friction velocity u_* .

The physical picture that emerges is very simple. In view of Lighthill's relation (6), mean spanwise vorticity $\bar{\omega}_z$ is generated at the two walls, at a rate given by $\partial\bar{p}/\partial x = -\gamma_*$. Due to the change in the direction of outward normal vector $\hat{\mathbf{n}}$, this vorticity is negative at $y = 0$ and positive at $y = 2h$. The negative vorticity at the bottom wall is transported upward and the positive vorticity at the upper wall is transported downward, leading to a constant negative mean vorticity flux $\bar{\Sigma}_{yz} = -\gamma_*$. Although the actual geometry and dynamics of vortex lines is quite complex (see subsections 3.2-3.3 below), what happens "on average" is that straight vortex lines are generated in the spanwise direction of equal strengths of vorticity, negative at the bottom and positive at the top. These then "cascade" toward the channel centerplane, where they annihilate each other.

It is interesting to compare the above with the more conventional picture of channel flow as a "momentum cascade" [1]. Integrating the mean x -momentum balance once in y gives a standard formula for the total stress, Reynolds stress plus viscous stress:

$$\bar{T}_{xy} = \overline{u'v'} - \nu \frac{\partial\bar{u}}{\partial y} = -u_*^2 \left(1 - \frac{y}{h}\right). \quad (16)$$

For $0 < y \ll h$, it follows that $\bar{T}_{xy} \approx -u_*^2$ (and likewise $\bar{T}_{xy} \approx u_*^2$ for $0 < 2h - y \ll h$), leading to the notion of a constant momentum flux range. In fact, however, $\bar{\Sigma}_{yz} = -\partial_y \bar{T}_{xy} = -u_*^2/h$, so that the stress can never be strictly constant in any range of y , whereas the vorticity flux is exactly constant $\bar{\Sigma}_{yz} = -\gamma_*$ over the whole channel cross-section.

The importance of the cross-stream flux of spanwise vorticity is that it is directly related to energy dissipation. By considering the balance equations of energy in the mean flow $(1/2)|\bar{\mathbf{u}}|^2$ and energy in the fluctuations $k = (1/2)\overline{|\mathbf{u}'|^2}$, it is easy to show that

$$\bar{u}_b \left(-\frac{\partial\bar{p}}{\partial x}\right) = \frac{1}{2h} \int_0^{2h} \left[\varepsilon(y) + \nu \left(\frac{\partial\bar{u}}{\partial y}\right)^2 \right] dy = \varepsilon_b^{\text{tot}}. \quad (17)$$

Here $\bar{u}_b = \frac{1}{2h} \int_0^{2h} \bar{u}(y) dy$ is the bulk velocity, averaged over a cross-section of the channel, and $\varepsilon(y) = \nu |\nabla \mathbf{u}'|^2$ is the “turbulent dissipation” (per unit mass) in the velocity fluctuations. To derive (17) we have used the result that turbulence production balances turbulent dissipation when integrated over the channel width:

$$\frac{1}{2h} \int_0^{2h} \left[-\overline{u'v'} \frac{\partial \bar{u}}{\partial y} \right] dy = \frac{1}{2h} \int_0^{2h} \varepsilon(y) dy.$$

The relation (17) can be rewritten by multiplication with the mass density ϱ as

$$\bar{J}_b(-\bar{\Sigma}_{yz}) = \varrho \varepsilon_b^{\text{tot}} \quad (18)$$

where $\bar{J}_b = \varrho \bar{u}_b$ is the mean mass flux through the pipe and $\varrho \varepsilon_b^{\text{tot}}$ is the bulk-average energy dissipation per unit volume. This relation shows the direct connection of vorticity flux with energy dissipation. As we shall see in Section 4, (18) is a special case of a far more general relation, valid for both classical and quantum fluids. The practical significance of (12), i.e. $\bar{\Sigma}_{yz} = \frac{\partial \bar{p}}{\partial x}$, and (18) is that both pressure-drop and energy dissipation can be reduced in turbulent flow by decreasing the cross-stream flux of spanwise vorticity. Any mechanism that interrupts the “vorticity cascade” will lead to turbulent drag reduction. Body-forces from electromagnetic forcing [21] and polymer additives [22, 23] are well-known devices.

In pipe flow, the relations (11) become

$$\overline{u'_r \omega'_\theta - u'_\theta \omega'_r} - \frac{\nu}{r} \frac{\partial}{\partial r} (r \bar{\omega}_\theta) = \bar{\Sigma}_{r\theta}^* = \frac{\partial \bar{p}^*}{\partial z} \quad (19)$$

$$\overline{u'_\theta \omega'_z - u'_z \omega'_\theta} = \bar{\Sigma}_{\theta z}^* = \frac{\partial \bar{p}^*}{\partial r} \quad (20)$$

$$\overline{u'_z \omega'_r - u'_r \omega'_z} = \bar{\Sigma}_{zr}^* = 0. \quad (21)$$

Similarly as before, $\bar{\Sigma}_{ij} = \bar{\Sigma}_{ij}^*$ for all i, j except $\bar{\Sigma}_{\theta z} = -\bar{\Sigma}_{z\theta} = -\bar{u}_z \bar{\omega}_\theta + \bar{\Sigma}_{\theta z}^*$ and $\frac{\partial \bar{p}^*}{\partial z} = \frac{\partial \bar{p}}{\partial z}$. The relation (19), or $\bar{\Sigma}_{r\theta} = \frac{\partial \bar{p}}{\partial z}$, is the crucial one. The radial-independence of the streamwise pressure-gradient follows from vorticity conservation:

$$\frac{\partial}{\partial r} \left(\frac{\partial \bar{p}}{\partial z} \right) = \partial_r \bar{\Sigma}_{r\theta} = 0.$$

The constant value $\frac{\partial \bar{p}}{\partial z} = -\gamma_*$ can be inferred from balancing the stress at the wall with the pressure-gradient applied across a cross-section of the pipe, i.e. $-2\pi r \cdot u_*^2 = \pi r^2 \cdot \frac{\partial \bar{p}}{\partial z}$ so that $\frac{\partial \bar{p}}{\partial z} = -\gamma_* = -2u_*^2/r$. The cascade picture “on average” is of vortex rings of positive azimuthal vorticity generated at the pipe wall and collapsing radially inward to annihilate at the axis.

3.2 Scaling Theories and Vortex Structures

The previous considerations have all been exact. We now develop additional insight using theoretical assumptions, involving scaling hypotheses and structural modeling. We consider explicitly only channel flow although the discussion applies as well to pipe flow.

3.2.1 Reynolds-Number Scaling Theories

We first examine the consequences of high-Reynolds number asymptotics. We shall discuss the classical asymptotic matching theory that leads to the logarithmic law of the wall, particularly as laid out in the review of Panton [26]. Many of the results that we deduce below from this theory can be obtained under more general assumptions, e.g. see [27, 28]. The classical theory has, however, the advantages of simplicity and familiarity, so that we shall restrict ourselves to it here. As usual, one introduces an inner scaling $y^+ = u_* y / \nu$, $\bar{u}^+ = \bar{u} / u_* = f(y^+, Re_*)$, $-\overline{u'v'}^+ = -\overline{u'v'} / u_*^2 = g(y^+, Re_*)$ with $Re_* = \frac{u_* h}{\nu} = h^+$. The stress relation (16) then becomes

$$g(y^+, Re_*) + \frac{\partial f}{\partial y^+}(y^+, Re_*) = 1 - \frac{y^+}{Re_*}.$$

The standard scaling hypothesis of the “law of the wall” is that $f(y^+, Re_*) \sim f_0(y^+)$ and $g(y^+, Re_*) \sim g_0(y^+)$ for $Re_* \gg 1$, and, in that case, $g_0(y^+) + f_0'(y^+) = 1$. Matching to an outer law leads to the prediction of a “logarithmic layer” with

$$f_0(y^+) \sim \frac{1}{\kappa} \ln y^+ + B, \quad g_0(y^+) \sim 1 - \frac{1}{\kappa y^+}$$

for $h^+ \gg y^+ \gg 1$. The above results are asymptotically valid only in the inner layer, with $y \ll h$. However, as discussed by Panton [26], these inner laws can be combined with outer laws

in a standard technique of “composite expansions” to yield high- Re_* asymptotic formulae that are uniformly valid over the whole channel width. In particular, a composite expansion for the Reynolds stress is

$$-\overline{u'v'}^+ \simeq g_0(y^+) - \frac{y^+}{Re_*} \quad (22)$$

As shown in [26], Fig.40, (22) is a very accurate approximation, even at rather low values of Re_* . This leads to an important consequence. Taking the derivative of $-\overline{u'v'}^+ \simeq 1 - \frac{1}{\kappa y^+} - \frac{y^+}{Re_*}$, one finds [26]

$$\frac{d}{dy^+}(-\overline{u'v'}^+) = \frac{1}{\kappa y^{+2}} - \frac{1}{Re_*}, \quad (23)$$

so that the peak of the Reynolds stress appears within the logarithmic layer at $y_p^+ \sim \sqrt{\frac{Re_*}{\kappa}}$ with maximum value $-\overline{u'v'}_p^+ \sim 1 - \frac{2}{\sqrt{\kappa Re_*}}$. This scaling of the location of the peak Reynolds stress has been well-verified empirically [29, 30, 31].

There are immediate implications for the turbulent vorticity flux, since, by the first line of (15), it is the derivative of the Reynolds stress: $\frac{\partial}{\partial y}(-\overline{u'v'}) = \overline{v'\omega'_z - w'\omega'_y}$. It follows that

$$\begin{aligned} \overline{v'\omega'_z - w'\omega'_y} &> 0 \text{ for } y^+ < y_p^+ \\ \overline{v'\omega'_z - w'\omega'_y} &< 0 \text{ for } y^+ > y_p^+. \end{aligned} \quad (24)$$

The condition of constant cross-stream vorticity flux which we derived in section 3 states that

$$\overline{v'\omega'_z - w'\omega'_y} - \nu \frac{\partial \overline{\omega}_z}{\partial y} = -\frac{u_*^2}{h} < 0.$$

The viscous term is negative over the whole channel width, since mean spanwise vorticity is negative at $y = 0$ and increasing monotonically to zero at $y = h$, so that $\partial \overline{\omega}_z / \partial y > 0$ for all y . However, the turbulent transport term is negative only for $y^+ > y_p^+$. These facts have been noted before [27, 28]. We restate them here in order to emphasize that *mean cross-stream transport of spanwise vorticity is dominated for $y^+ < y_p^+$ by viscous diffusion*, which gives the contribution of largest magnitude. This result does not contradict any of the assumptions in the derivation of the log-layer—and indeed is a consequence of that derivation—but it does contradict a common belief that “the overall dynamics of turbulent boundary layers is independent of viscosity” [1].

Further insight can be obtained by considering the constant-flux condition in inner-scaling:

$$\overline{v'\omega'_z - w'\omega'_y}^+ - \frac{\partial \overline{\omega}_z^+}{\partial y^+} = -\frac{1}{Re_*},$$

with

$$\overline{v'\omega'_z - w'\omega'_y}^+ = g'(y^+, Re_*), \quad \partial \overline{\omega}_z^+ / \partial y^+ = -f''(y^+, Re_*).$$

Right at the wall, $g'(0, Re_*) = -1/Re_*$ and $f''(0, Re_*) = 0$, so that the vorticity transport is entirely due to viscous diffusion in close vicinity of the wall. In the range $1 \ll y^+ < y_p^+$ the two functions g' , f'' are of order unity, so that the small difference $-1/Re_*$ must be due to near-cancellation of almost equal quantities. Thus, the viscous and turbulent transport of vorticity are both relatively large and the negative residual value of the cross-stream flux is due to a slight dominance of the viscous transport. It is only for $y^+ \gtrsim y_p^+$ that the turbulent transport dominates and that one can properly think of an “inertial sublayer” dominated by nonlinear interactions. For more discussion of these points, see [27, 28].

One of the consequences of these considerations is that the mean velocity profile $\bar{u}(y)$ plays a critical role in the vorticity cascade over the range $y < y_p$, since the viscous flux equals $\nu d^2 \bar{u}(y)/dy^2$. Conversely, the statistics of vorticity production and transport at the boundary are a crucial factor in determining the mean profile; for instance, see [32]. This may have significant implications on understanding the mechanism of polymer drag-reduction [22, 23], for example. As can be seen from the general expression (10), mean vorticity flux for turbulent pipe flow with a polymer additive will consist of three distinct contributions: the nonlinear turbulent transport, viscous transport, and direct transport by Magnus effect of polymeric forces. Given the known drag-reduction effects of polymers, it follows from our discussion that wall-normal vorticity flux must also be drastically reduced by polymer additives. However, this may occur *a priori* in several possible ways. For example, for $y < y_p$ either the viscous transport may decrease in magnitude or the turbulent transport (which is of opposite sign) may increase in magnitude. Further research will be necessary to see which of these possibilities is realized.

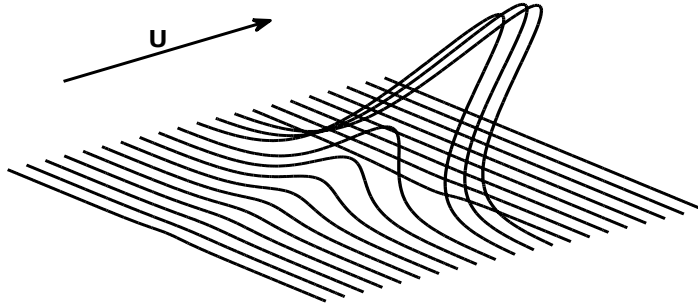


Figure 1: A horseshoe vortex bundle as originally conceived by Theodorsen (1952).

3.2.2 Vortex Structure Models

Our previous discussion has emphasized the importance of understanding the structure and dynamics of vorticity in pipe and channel flow. There have indeed been many proposals to explain and model the physics of wall-bounded shear flows in terms of typical vortex structures. One of the earlier attempts was that of Theodorsen [33], who suggested that the most significant structures are “horseshoe vortices” inclined at 45° to the wall, which form by roll up of streamwise vorticity in the viscous sublayer. See Fig. 1. Considerable evidence has been found in support of horseshoe vortices (also known as hairpin, Λ and Ω vortices) from both experiment and numerical simulation [34, 35, 36, 37, 38, 39]. However, many other alternative proposals have been made. To quote from a review of Fiedler [37]: “Thus, when studying the literature on boundary layers, one is soon lost in a zoo of structures, e.g. horseshoe- and hairpin-eddies, pancake- and surfboard-eddies, typical eddies, vortex rings, mushroom-eddies, arrowhead-eddies, etc ...”. It is fair to say that no clear consensus has emerged as to which vortex structures are the most relevant to the dynamics and statistics of the turbulence.

Most of the effort in identifying coherent-vortices and in constructing vortex models of the turbulent boundary layer has gone into explaining their contribution to the Reynolds stress. The importance of maintaining a (nearly) constant Reynolds stress across the “inertial sublayer” has

been widely recognized. However, almost no effort has been made to explain the cross-stream transport of spanwise vorticity in terms of typical vortex structures. (But see [5, 6, 7, 8, 9], discussed more below.) Furthermore, the fundamental constraint of maintaining a constant mean vorticity flux across the pipe or channel has been almost universally ignored.

Here we shall discuss such issues in the context of the “hairpin vortex” model of Perry, Chong and collaborators [40, 41, 42, 43, 44]. This model is one of the most fully articulated attempts to explain, in analytical terms, the features of the turbulent boundary-layer by means of representative vortex-structures. The Perry-Chong (PC) theory combines the Theodorsen proposal [33] of “horseshoe” or “hairpin” vortices with Townsend’s “attached eddy hypothesis” [45]. In this picture, the boundary layer consists of a scale-invariant hierarchy of hairpin-like structures, which are attached to the wall in the sense that their characteristic lengths are proportional to the distance at which the eddy extends above the wall. By averaging over an ensemble of such structures, the PC theory yields important quantitative results, such as a logarithmic mean velocity profile and constant Reynolds stress in the overlap region, profiles of normal Reynolds stresses, tensor energy spectra as functions of distance from the wall, etc.

PC theory is sufficiently developed that the turbulent contribution to vorticity flux $\overline{\Sigma_{yz}^{turb}} = \overline{v'\omega'_z - w'\omega'_y}$ may be calculated by evaluating each term separately, e.g. as integrals in wavenumber over the model energy spectra. However, for our purposes a simpler approach suffices, which is to use again the identity $\frac{\partial}{\partial y}(-\overline{u'v'}) = \overline{v'\omega'_z - w'\omega'_y}$. We may start from the PC formula for the Reynolds stress as an average over hierarchy lengths δ , e.g. equation (27) in [42]:

$$\overline{u'_i u'_j} = u_*^2 \int_{\delta_1}^{\Delta_E} I_{ij} \left(\frac{y}{\delta} \right) p_H(\delta) d\delta \quad (25)$$

Here $\delta_1 = O(\nu/u_*)$ is the length-scale of the smallest hierarchy, whereas $\Delta_E = O(h)$ is the length-scale of the largest. The function $I_{ij}(y^*)$ is obtained by integrating over spectra of the representative vortex structures. See also Townsend [45], who referred to $I_{ij}(y^*)$ as an “eddy-intensity function.” Both PC and Townsend required a distribution of hierarchy lengths $p_H(\delta) = M/\delta$ for $\delta_1 < \delta < \Delta_E$ in order to reproduce a logarithmic mean velocity profile and

a constant Reynolds stress. We may follow their arguments to study also the derivative of the stress, e.g. see [40], Appendix B. Thus, changing integration variable to $y^* = y/\delta$

$$\overline{u'_i u'_j} = Mu_*^2 \int_{y/\delta_1}^{y/\Delta_E} I_{ij}(y^*) \frac{dy^*}{y^*}.$$

and then differentiating gives

$$\frac{d}{dy} \overline{u'v'} = \frac{Mu_*^2}{y} \left[I_{xy} \left(\frac{y}{\delta_1} \right) - I_{xy} \left(\frac{y}{\Delta_E} \right) \right]. \quad (26)$$

Using the result $I_{xy}(y^*) \rightarrow 0$ for $y^* \gtrsim 1$ and $I_{xy}(y^*) \sim -Qy^*$ for $y^* \ll 1$ [40] gives

$$\overline{v'\omega'_z - w'\omega'_y} = \frac{d}{dy} (-\overline{u'v'}) \approx -\frac{MQu_*^2}{\Delta_E}$$

for $\delta_1 \lesssim y \ll \Delta_E$. This same result may also be obtained by differentiating the final result for the Reynolds stress in Appendix B of [40]. Since $\Delta_E = O(h)$, the PC theory yields a constant of the correct order, $\overline{v'\omega'_z - w'\omega'_y}^+ = O(1/Re_*)$.

These results appear satisfactory, but a little thought shows that the PC theory is adequate to explain vorticity flux only over the range $y_p^+ < y^+ \ll h^+$, in the notations of the previous subsection. It is only over that range that the *turbulent* vorticity flux is constant and, otherwise, the viscous diffusion is dominant. To obtain the correct negative sign of the turbulent flux over the range $y_p^+ < y^+ \ll h^+$ (and also to obtain the correct sign of the Reynolds stress [40]), the constant Q in the above calculation must be positive. However, as we have seen in the previous subsection, the turbulent vortex flux must reverse sign and become positive for $0 < y^+ < y_p^+$. The PC theory, as it is presently constituted, is inadequate to explain this sign-reversal. This is not a failure just in the buffer layer but over half of the range of the traditional log-layer.

Let us consider briefly one possible remedy. As mentioned above, it has usually been assumed in the PC model that $I_{xy}(y^*) = 0$ for $y^* \gtrsim 1$. For example, see Figure 14 of [41] or Figure 4 of [42], where $I_{xy}(y^*) = 0$ for $y^* \geq 1$. This corresponds to the severe assumption that vortex hierarchy elements of length-scale δ make no contribution to Reynolds stress at wall-normal distances $y > \delta$. If one hypothesizes instead a slow power-law decay of the precise

form $I_{xy}(y^*) \sim -\frac{P}{y^*}$, $y^* \gg 1$, with P another universal, positive constant, then (26) yields

$$\frac{d}{dy}(-\overline{u'v'}) = Mu_*^2 \left(P \frac{\delta_1}{y^2} - \frac{Q}{\Delta_E} \right)$$

for $\delta_1 \ll y \ll \Delta_E$, in qualitative agreement with eq.(23). The agreement becomes exact for a suitable choice of the constants M, P, Q . An interesting problem for future investigation might be to determine which “representative” vortex structures, if any, lead to the necessary -1 power-law decay of the eddy-intensity function $I_{xy}(y^*)$ for $y^* \gg 1$.

3.3 Experiments and Simulations

It would be very useful to get some additional clues from experiment and simulation. There seem, however, to be very few empirical studies of the turbulent vorticity flux or its relevant constituent averages, $\overline{v'\omega'_z}$ and $\overline{w'\omega'_y}$. We know of no experimental measurements at all for turbulent flow in pipes or ducts. The most exhaustive investigations have been carried out in zero-pressure turbulent boundary layers, by Klewicki and collaborators. Those studies include wind-tunnel boundary layers with $Re_\theta = 1010 \sim 4850$ [5, 6] and atmospheric boundary layers with $Re_\theta = 2 \sim 4 \times 10^6$ [7]. We also know of only two studies of these velocity-vorticity correlations by direct numerical simulation of channel flow, the $Re_* = 250$ calculation of Leighton & Handler reported by Bernard [9] and a $Re_* = 200$ DNS of Crawford & Karniadakis [21].

The picture which emerges from the lower Reynolds-number studies [5, 6, 9, 21] is as follows:

$$\begin{aligned} \overline{v'\omega'_z} &> 0 > \overline{w'\omega'_y} \quad \text{for } y^+ < 12 \\ 0 &> \overline{v'\omega'_z} > \overline{w'\omega'_y} \quad \text{for } 12 < y^+ < y_p^+ \\ 0 &> \overset{?}{\overline{w'\omega'_y}} > \overline{v'\omega'_z} \quad \text{for } y^+ > y_p^+ \end{aligned}$$

A question mark is included in the last line since the DNS of [9, 21] indicates that $\overline{w'\omega'_y}$ becomes slightly positive for $y^+ \gtrsim 50 > y_p^+ \simeq 30$. The results for $y^+ > y_p^+$ agree rather well with the physical picture of vortex dynamics in the PC model [40]: “the Λ -vortex stretches under its own mutual induction with its image to give, in the large, plane strain ... The plane strain

brings the legs of the vortex together". The lifting of the negative streamwise vorticity in the head and legs of the hairpin produces $\overline{v'\omega'_z} < 0$. The simultaneous collapse of the hairpin legs towards each other, carrying opposite signs of wall-normal vorticity, produces $\overline{w'\omega'_y} < 0$. The slight positive value of $\overline{w'\omega'_y}$ for larger y values has been interpreted by Bernard [9] also in terms of hairpin structures, as due to the reversal of w' at some height above the counter-rotating legs of the vortex. Our calculation in the previous subsection indicates that $\overline{w'\omega'_y} > \overline{v'\omega'_z}$, yielding a net negative vorticity flux. For more detailed discussion of these correlations in terms of typical vortex structures, see [6], Section III and [9], Section 4.

On the other hand, the PC model does not seem to accord well with the lower Reynolds observations for $y^+ < y_p^+$. Klewicki et al. [6] have made a detailed quadrant analysis of the contributions to $\overline{v'\omega'_z}$ at $y^+ = 5.3, 14.2$ and 26.3 in the BL at $Re_\theta = 1010$ with $y_p^+ \doteq 40$. Although $\overline{v'\omega'_z} < 0$ for $y^+ = 14.2$ and 26.3 , as the hairpin picture might suggest, [6] have found that the dominant events are 2nd-quadrant, i.e. $v' < 0$ and $\omega'_z > 0$. Furthermore there is strong dependence on Reynolds number, with the magnitude of $\overline{v'\omega'_z}$ decreasing sharply with increasing Reynolds number for $Re_\theta = 1010 \sim 4850$.

These tendencies persist in the high Re_θ data from the ABL in [7]. In fact, their smooth-wall data at $Re_\theta = 2 \times 10^6$ show $\overline{v'\omega'_z} > 0$ for the whole range of y^+ . Furthermore, $\overline{w'\omega'_y}$ appears to change sign, being negative for $y^+ < y_p^+$ and positive for $y^+ > y_p^+$ (using rough-wall data). The sign for $y^+ > y_p^+$ may be due to growth of hairpin vortices in the spanwise direction [39, 46, 47]. Clearly, further experimental and numerical studies would be most helpful, in order to verify the limited data and to map out all the dependencies on wall-distance, Reynolds number, roughness, etc. Particularly illuminating would be conditional sampling studies, with VISA (variable-interval space-averaging) sampling technique and quadrant conditions like those applied to Reynolds stress [35, 36], but now carried out for the vorticity flux. Such investigations could help to reveal the vortex structures and dynamics which contribute most significantly to the cross-stream transport of spanwise vorticity.

4 Comparison of Classical and Quantum Fluids

We shall now discuss briefly some of the corresponding problems in the field of quantum superfluids. A complete review of superfluidity and superconductivity would be out of place here and we refer the reader interested in further background to standard texts [48, 49]. We just remark on a few basic facts, the most important of which is quantization. As first noted by Onsager [50] and Feynman [51], the vorticity in neutral superfluids resides entirely in thin filaments whose circulation is quantized in units of $\kappa = h/m$, where h is Planck's constant and m is the atomic mass of the condensed Bose particle. For liquid ${}^4\text{He}$, $\kappa \approx 9.97 \times 10^{-4} \text{ cm}^2/\text{sec}$ and the core radius of the vortex lines is of order of angstroms. An analogous fact holds for charged superfluids or superconductors, in which the condensed Bose "particle" is generally a Cooper pair of two electrons of charge $2e$. As first pointed out by London [52], the magnetic flux in a superconductor is likewise quantized in units of $\Phi_0 = h/2e = 2.07 \times 10^{-15} \text{ webers}$. London considered what are now called "Type-I superconductors" which are perfect diamagnets and expel all magnetic fields (the Meissner effect). Thus, he had in mind the magnetic flux through superconducting rings and other non-simply-connected samples. However, it was pointed out later by Abrikosov [53, 54] that there is another class of "Type-II superconductors" which are penetrated by magnetic flux tubes with flux quantized in units of Φ_0 .

We now discuss the "phase-slip" phenomenon, which is closely analogous to the results for classical turbulence presented in section 2.3. These ideas were first employed by Josephson for superconductors and extended further for both superfluids and superconductors by Anderson, hence often called the "Josephson-Anderson relation" [13]. The classic presentation is in the review article by Anderson [10]. He argued there that the drop in chemical potential μ (per unit mass) between two points P_1 and P_2 in a neutral superfluid should be related to the rate dn/dt at which quantized vortex-lines cross an oriented line between the two points:

$$\overline{\mu(P_2)} - \overline{\mu(P_1)} = \kappa \overline{dn/dt} \quad (27)$$

Here the overbar indicates a time-average. In an appendix—entitled "A 'New' Corollary in

Classical Hydrodynamics?”—Anderson also pointed out that this relation for quantum fluids has a precise classical analogue, of the form:

$$\overline{\left(p + U + \frac{1}{2}|\mathbf{u}|^2\right)}_{P_2} - \overline{\left(p + U + \frac{1}{2}|\mathbf{u}|^2\right)}_{P_1} = \int_{P_1}^{P_2} \overline{\mathbf{u} \times \boldsymbol{\omega} \cdot d\mathbf{x}}. \quad (28)$$

This is just the relation (9) that we derived earlier, in the special case of an inviscid fluid, with no body-forces, and in line-integral form. It is a generalization of the relation noted by Taylor [4] for shear turbulence. A similar relation can be obtained for type-II superconductors

$$\overline{V(P_2)} - \overline{V(P_1)} = \Phi_0 \overline{dn/dt}, \quad (29)$$

now relating the difference in voltage between two points to the rate at which a line from P_1 to P_2 is crossed by quantized flux [55, 56]. This relation was the basis of Anderson’s “flux-creep theory” to explain resistive behavior in type-II superconductors above a critical current.

These ideas were perhaps most carefully elaborated by Huggins [11]. His paper is especially interesting for us, because he employed the classical fluid equations as his model, despite intended applications to quantum superfluids. This is legitimate, because a superfluid will obey the laws of classical hydrodynamics except close to the cores of vortex lines. Huggins makes several assumptions that are adapted to the superfluid problem, e.g. that all the vorticity is confined to compact vortex tubes with total circulation of magnitude κ . However, almost all of his discussion can be easily generalized to the case of continuous vorticity distributions of any magnitude (see Appendix B).

The starting point of Huggin’s treatment is Kelvin’s minimum kinetic energy theorem [57]. As is well-known, Kelvin showed that, among all incompressible velocity fields with the same boundary conditions in a finite domain Ω , the one with minimum energy is the potential flow. To prove this, Kelvin decomposed the velocity field as $\mathbf{u} = \mathbf{u}_\phi + \mathbf{u}_\omega$ where $\mathbf{u}_\phi = \nabla\phi$ is the potential flow with the specified inflow-outflow boundary conditions and \mathbf{u}_ω is a field containing all of the vorticity of the fluid but with no flow through the boundary. In that case the kinetic energy decomposes into a sum of kinetic energies for the potential and vortex fields, so that

$E = E_\phi + E_\omega \geq E_\phi$. Huggins discusses a classical fluid model in the form

$$\partial_t \mathbf{u} = -\nabla h + \mathbf{u} \times \boldsymbol{\omega} + \mathbf{g}, \quad (30)$$

where the enthalpy $h = p + U + \frac{1}{2}|\mathbf{u}|^2$ includes the contribution of any potential energy U whereas \mathbf{g} contains all the non-potential forces, e.g. $\mathbf{g} = -\nu(\nabla \times \boldsymbol{\omega}) + \mathbf{f}$ if there is only a viscous force and a non-conservative body-force. Huggins further considers flow through a channel driven by a difference in the enthalpy h_{in} at the inflow section and enthalpy h_{out} at the outflow section. In this setting [11] proves that

$$\dot{E} = J(h_{in} - h_{out}) + \int_{\Omega} \varrho \mathbf{u} \cdot \mathbf{g} d^3x \quad (31)$$

$$\dot{E}_\phi = J(h_{in} - h_{out}) - \kappa \dot{J}_\phi \quad (32)$$

$$\dot{E}_\omega = \kappa \dot{J}_\phi + \int_{\Omega} \varrho \mathbf{u} \cdot \mathbf{g} d^3x \quad (33)$$

Let us consider each of these relations in turn.

The first result (31) is just the standard energy balance relation. Since J is the total mass flux through the pipe, $J(h_{in} - h_{out})$ equals the energy input into the fluid through work by the applied enthalpy difference. On the other hand, $D = -\int_{\Omega} \varrho \mathbf{u} \cdot \mathbf{g} d^3x$ just represents the dissipation by the non-potential forces. The second relation (32) is more interesting. This result shows that the energy supplied by the enthalpy difference goes entirely into the potential flow. What acts as “dissipation” on the potential flow is the term $\kappa \dot{J}_\phi$, which transfers energy to the vortex system. As seen from the final relation (33), this energy is then dissipated by the non-potential forces, e.g. ordinary viscosity, acting on the vortices. The transfer term is the product of the quantum of circulation κ and the rate \dot{J}_ϕ at which vortex lines are crossing the mass flux in the potential flow. For example, for a single length of vortex line

$$\kappa \dot{J}_\phi = \kappa \int_{vort} \varrho \mathbf{u}_\phi \cdot \mathbf{u}_v \times d\mathbf{l} \quad (34)$$

The quantity \mathbf{u}_v is the velocity of the element $d\mathbf{l}$ of vortex line, so that $\mathbf{u}_v \times d\mathbf{l}$ represents the rate at which the line-element sweeps out area. It is easy to recover Anderson’s relation (27) [or

(28)] from (32). For example, if vortex lines are crossing the entire mass flux J in the channel at a frequency ν , then $\dot{J}_\phi = J\nu$. In that case, $h_{in} - h_{out} = \kappa\nu$ for steady-state flow.

Note that it is crucial in (34) that $\mathbf{u}_v \neq \mathbf{u}_\phi$, or otherwise $\dot{J}_\phi = 0$. Thus, it is important that quantized vortex lines are *not* material lines, moving with the local potential velocity \mathbf{u}_ϕ . An analogous fact is true for vortex lines in classical flow which, because of the non-potential force \mathbf{g} , do not move with the local fluid velocity \mathbf{u} . In general one may decompose the non-potential force into components transverse and longitudinal to the local vorticity vector:

$$\mathbf{g} = \Delta\mathbf{u} \times \boldsymbol{\omega} + \alpha\boldsymbol{\omega}, \quad (35)$$

where $\Delta\mathbf{u} = \boldsymbol{\omega} \times \mathbf{g} / |\boldsymbol{\omega}|^2$, $\alpha = \boldsymbol{\omega} \cdot \mathbf{g} / |\boldsymbol{\omega}|^2$. The vector $\Delta\mathbf{u}$ can be interpreted as a “drift velocity” of vortex lines with respect to the local fluid velocity, so that the vortex line moves with net velocity $\mathbf{u}_v = \mathbf{u} + \Delta\mathbf{u}$. In that case, the transverse force has the form of a “Magnus force” $(\mathbf{u}_v - \mathbf{u}) \times \boldsymbol{\omega}$, similar to that which acts on superfluid vortices [58, 59]. On the other hand, there are non-vanishing longitudinal forces as well in classical fluids and these lead to non-trivial effects, such as helicity cascade [60] and kinematic α -effect [61]. The effect of both terms on vortex motion is clearly seen in turbulent flows, where viscosity leads to quite different properties of material lines and vortex lines [62]. These effects appear to persist even in the zero-viscosity limit, when vortex lines behave as material lines only in an average sense [63, 64].

It is interesting to note that the phase-slips of quantized flux lines and their consequent dissipation lead to a “drag reduction problem” in superconductor technology. In type-II superconductors the result analogous to Huggins’ above is that crossing of supercurrent by flux lines at a rate \dot{I}_ϕ produces an energy dissipation $I(V_1 - V_2) = \Phi_0 \dot{I}_\phi$, where I is the total electric current. This motion of vortices produces a “quasi-resistance” in type-II superconductors above some critical current I_c , which destroys their useful superconducting properties. This problem is particularly severe for the newer class of high-temperature superconductors (HTS), since the vortices there are subject to weaker restoring forces and stronger thermal fluctuations. Unlike the vortices in conventional type-II superconductors which are frozen into an Abrikosov

lattice or vortex crystal, the vortices in HTS melt at high enough temperatures into a mobile “vortex liquid” that produces sizable resistivity. See [65, 66, 67] and, for an excellent popular account, [68]. One solution to this problem is to “pin” the vortices to prevent their motion. Methods that have proved successful in more conventional type-II superconductors are to dope the superconductor with impurities or to manufacture wires and films from sintered powders (e.g. see [69, 70] as representative papers). Anything that prevents free cross-current motion of the quantized vortices restores the superconducting properties and permits electric current to flow with no resistance.

An even closer analogy exists between classical turbulence and turbulence in neutral superfluids, as originally conceived by Feynman [51]. To quote his own words:

“In ordinary fluids flowing rapidly and with very low viscosity the phenomenon of turbulence sets in. A motion involving vorticity is unstable. The vortex lines twist about in an ever more complex fashion, increasing their length at the expense of the kinetic energy of the main stream. That is, if a liquid is flowing at a uniform velocity and a vortex line is started somewhere upstream, this line is twisted into a long complex tangle further downstream. To the uniform velocity is added a complex irregular velocity field. The energy for this is supplied by pressure head. We may imagine that similar things happen in the helium.” —Feynman (1955)

Experiments on turbulent flow of superfluid ^4He in circular pipes [71] and rectangular ducts [72] show similar behaviors as classical turbulence, both in drag resistance as functions of Reynolds number and in mean velocity profiles. In addition to the complex, random motion of vortex lines discussed by Feynman above, there must also be organized motion. Just as in the classical case, there must be a “cascade” of azimuthal vorticity along the radial direction toward the pipe axis. As follows from our discussion above, this is essential for the vortex lines to extract energy from the pressure head. Vortex structures like “hairpins,” “rings,” etc. will also doubtless form and contribute to the necessary cross-stream flux of vorticity.

5 Discussion and Conclusions

We have presented in this paper a systematic picture of pressure-driven turbulence in pipes and channels as spatial “inverse cascades” of spanwise vorticity in the cross-stream direction. This complements the more conventional picture of these flows as “forward cascades” of streamwise momentum, also across the stream but toward the viscous layer at the wall. Following Huggins [14], we have shown that the spatial flux of vorticity is necessary to produce a pressure-drop down the pipe and consequent dissipation. This flux is dominated by viscous diffusion of vorticity at distances to the wall less than the peak of the Reynolds stress, well into the classical log-layer. The Perry-Chong model based on “representative” hairpin/horsehoe vortices has been shown to be inadequate to describe the cross-stream vorticity flux over that range, but viable at distances greater than the Reynolds-stress maximum. We have shown that similar results hold for quantum superconductors and superfluids, and, especially, for superfluid turbulence driven by applied pressure gradients in pipes and channels.

We hope that one consequence of this work will be to stimulate a greater effort by experimentalists and numericists to discover the detailed vortex structures and dynamics which contribute to the cross-stream vorticity transport, as a function of distance to the wall and of Reynolds number. Theorists should also recognize the condition of constant wall-normal vorticity flux as an important constraint on statistical models and closures. On the practical side, we cannot emphasize too strongly that *pressure-drop and cross-stream transport of spanwise vorticity are mathematically equivalent*. This is a very universal fluid-dynamical result, applicable not only to turbulence but also to laminar and transitional flow. See eqs. (32),(33) or the very general formulation in eq. (39) of Appendix B, for instance. In fully-developed turbulence in channels and pipes, which enjoys all the statistical symmetries permitted by the boundary conditions, this dynamical constraint leads to constant time-average flux of spanwise vorticity across the main flow. The laminar solution in channel geometry with parabolic velocity profile has also a constant vorticity-flux, given entirely by viscous transfer (see [14], section 13). In

the turbulent case, there is an additional mean contribution from nonlinear transport. For a fixed mass-flux, the vorticity transfer in turbulent flow is much greater than in the laminar state, leading to a greatly enhanced streamwise pressure drop and enhanced energy dissipation. Any method for reducing drag must therefore reduce the cross-stream transfer of vorticity. It is hoped that the vortex-cascade framework presented here will provide new perspectives on the difficult problems of wall-bounded turbulence.

A fresh view of the role of the vorticity may be of use, in particular, in the problem of polymer drag reduction. It has long been suspected that the critical action of polymers in turbulent drag reduction is through their interaction with vortices [22, 23, 73]. The same is also true for various other drag-control strategies, such as with electromagnetic body forces [21]. A persistent puzzle has been to understand how polymer-induced changes in vortex structure are mediated into substantial changes of the large-scale structure of the flow. The vorticity flux tensor (8) is a natural locus for critical polymer activity. There is generally a scale separation in high Reynolds number turbulence between the peaks of the spectra of the velocity and the vorticity. However, [7] have found that the velocity-vorticity cospectra in boundary layers are not generally dominated by intermediate wavenumbers between these two peaks, but instead get dominant contributions from wavenumbers near the peak in the associated vorticity spectra and, in some cases, also near the peak in the associated velocity spectra. Thus the velocity-vorticity correlations that contribute to the turbulent vorticity flux are a natural bridge between the small-scale and large-scale features of the flow.

Acknowledgements. I thank C. Barenghi, P. Bernard, S. Chen, P. Hohenberg, J. Klewicki, A. Leonard, C. Meneveau, S. Pope, K. Sreenivasan and J. Wallace for discussions. I am particularly grateful to P. Ao for suggesting a connection between turbulent dissipation and the Josephson-Anderson relation in superfluids. I also thank R. J. Adrian for helping to stimulate my early interest in turbulent boundary layers and their vortical structures. This work was supported by NSF grant # ASE-0428325 at the Johns Hopkins University and by the Center for Nonlinear Studies at Los Alamos National Laboratory.

A Appendix: The Vorticity Source Density at a Wall

It is the purpose of this appendix to derive the following expression

$$\boldsymbol{\sigma} = \hat{\mathbf{n}}' \times [\nu \nabla \times \boldsymbol{\omega} - \mathbf{f}]$$

for the vorticity source density at the wall. Here, in contrast to the main text, we have preferred to use the *inward*-pointing unit normal $\hat{\mathbf{n}}' = -\hat{\mathbf{n}}$ at the boundary $\partial\Omega$ of the domain. Let us consider any unit vector \mathbf{e}_i locally tangent to the surface, $\hat{\mathbf{n}} \cdot \mathbf{e}_i = 0$, and consider the small square loop C normal to \mathbf{e}_i , with one edge lying in the boundary surface $\partial\Omega$:

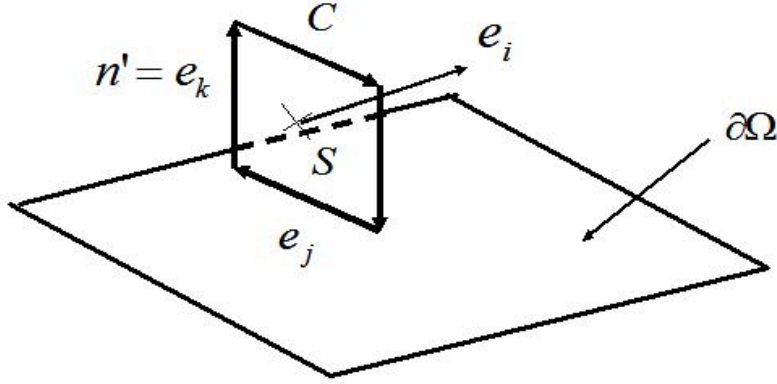


Figure 2: A test loop orthogonal to the wall.

Here, $\mathbf{e}_i \times \mathbf{e}_j = \mathbf{e}_k = \hat{\mathbf{n}}'$ and the edge tangent to \mathbf{e}_j lies in the surface $\partial\Omega$. If S is the square surface bounded by C ,

$$\int_S \omega_i dx_j dx_k = \oint_C \mathbf{u} \cdot d\mathbf{x}.$$

Letting $S(t)$ and $C(t)$ be the surface S and loop C materially advected by the fluid, then by the Kelvin Theorem

$$\frac{d}{dt} \int_{S(t)} \omega_i dx_j dx_k |_{t=0} = \frac{d}{dt} \oint_{C(t)} \mathbf{u}(t) \cdot d\mathbf{x} |_{t=0} = \oint_C [-\nu \nabla \times \boldsymbol{\omega} + \mathbf{f}] \cdot d\mathbf{x}.$$

The bottom segment parallel to \mathbf{e}_j —which is stationary in the surface because of the stick conditions—contributes a term

$$\int_{C \cap \partial\Omega} [-\nu \nabla \times \boldsymbol{\omega} + \mathbf{f}]_j dx_j$$

to the time-derivative of the flux $\int_S \omega_i dA$. We therefore identify

$$\sigma_i = -\nu(\nabla \times \boldsymbol{\omega})_j + f_j$$

or, for any direction,

$$\boldsymbol{\sigma} = \hat{\mathbf{n}}' \times [\nu \nabla \times \boldsymbol{\omega} - \mathbf{f}],$$

in agreement with our earlier finding.

The above argument also reveals the precise meaning of the “vorticity source density” $\boldsymbol{\sigma}$. If one considers any loop C with part of its length in the boundary $\partial\Omega$, then the contribution of the boundary segment to the time-derivative of the vorticity flux through C is given by

$$\int_{C \cap \partial\Omega} \boldsymbol{\sigma} \cdot (\hat{\mathbf{t}} \times \hat{\mathbf{n}}') ds$$

where $\hat{\mathbf{t}}$ is the unit tangent vector along the curve C , for a specified orientation. With this convention the flux is measured positive in the direction to the righthand side as one traverses the curve C , i.e. parallel to $\hat{\mathbf{t}} \times \hat{\mathbf{n}}'$.

The expression that we have derived for the “vorticity source density”

$$\boldsymbol{\sigma} = \hat{\mathbf{n}}' \times [\nu \nabla \times \boldsymbol{\omega} - \mathbf{f}]$$

is the same as that obtained by Lyman [15]. There seems, however, to be some controversy about this result. It has been argued by Wu & Wu [17] that Lyman’s prescription (and ours!) is incorrect and they suggest that $\hat{\mathbf{n}}' \times \nu(\nabla \times \boldsymbol{\omega})$ be replaced instead with

$$\boldsymbol{\sigma}_{\text{Wu}} = \nu \frac{\partial \boldsymbol{\omega}}{\partial n} = \nu(\hat{\mathbf{n}} \cdot \nabla) \boldsymbol{\omega}$$

with outward-pointing normal $\hat{\mathbf{n}}$. The two expressions have equal integrals over the boundary $\partial\Omega$ of the flow-domain since, by the divergence theorem and vector-calculus identities, they

both equal $\int_{\Omega} \nu \nabla^2 \boldsymbol{\omega} d^3x$. The two differ locally by a term $(\nabla \hat{\mathbf{n}})\boldsymbol{\omega}$, which vanishes for a flat surface. In particular, the two expressions agree for channel flow. However, with the precise interpretation of the vorticity source density given by us above, our result is a direct consequence of the Kelvin Theorem. We note furthermore that $\boldsymbol{\sigma}$ ought to lie parallel to vorticity vectors generated within the boundary surface and thus satisfy $\hat{\mathbf{n}} \cdot \boldsymbol{\sigma} = 0$. While Lyman's prescription always satisfies this condition, that of Wu & Wu does not in general.

B Appendix: The Detailed Josephson Relation

We present here a proof of the ‘‘detailed Josephson relation,’’ due to Huggins [11]. Although all of the results presented below are essentially contained in his paper, the generality of those results is somewhat obscured by various special assumptions invoked in that work. Our derivation has a slight novelty and hopefully makes the main ideas more clear.

We consider a generalized channel geometry, where the simply-connected flow domain Ω has boundary consisting of an in-flow surface S_{in} , an out-flow surface S_{out} , and wall surface S_w . The boundary conditions on the velocity \mathbf{u} are:

$$\mathbf{u}|_{S_{in}} = \mathbf{u}_{in}, \quad \mathbf{u}|_{S_{out}} = \mathbf{u}_{out}, \quad \mathbf{u}|_{S_w} = \mathbf{0}. \quad (36)$$

Huggin's argument builds upon the proof of the Kelvin minimum-energy theorem [57]. Thus, the velocity is decomposed as $\mathbf{u} = \mathbf{u}_{\phi} + \mathbf{u}_{\omega}$, where $\mathbf{u}_{\phi} = \nabla \phi$ is the unique potential flow field satisfying the incompressibility constraint $\nabla \cdot \mathbf{u}_{\phi} = \Delta \phi = 0$ and the through-flow boundary conditions

$$\hat{\mathbf{n}} \cdot \mathbf{u}_{\phi}|_{S_{in}} = \hat{\mathbf{n}} \cdot \mathbf{u}_{in}, \quad \hat{\mathbf{n}} \cdot \mathbf{u}_{\phi}|_{S_{out}} = \hat{\mathbf{n}} \cdot \mathbf{u}_{out}, \quad \hat{\mathbf{n}} \cdot \mathbf{u}_{\phi}|_{S_w} = \mathbf{0}, \quad (37)$$

inherited from the full velocity \mathbf{u} . Thus, $\mathbf{u}_{\omega} = \mathbf{u} - \mathbf{u}_{\phi}$ is also incompressible, carries the full vorticity of the flow ($\boldsymbol{\omega} = \nabla \times \mathbf{u}_{\omega}$), and satisfies the no-through b.c. $\hat{\mathbf{n}} \cdot \mathbf{u}_{\omega}|_{\partial\Omega} = 0$. It follows from these facts that

$$\int_{\Omega} \mathbf{u}_{\phi} \cdot \mathbf{u}_{\omega} d^3x = \int_{\Omega} \nabla \cdot [\phi \mathbf{u}_{\omega}] d^3x = \int_{\partial\Omega} \phi \mathbf{u}_{\omega} \cdot \hat{\mathbf{n}} dA = 0.$$

This orthogonality of \mathbf{u}_ϕ and \mathbf{u}_ω is, of course, the essence of Kelvin's theorem.

One can now substitute $\dot{\mathbf{u}}_\phi = \nabla \dot{\phi}$ into the equation of motion (30) to obtain an equation for the time-derivative of \mathbf{u}_ω :

$$\dot{\mathbf{u}}_\omega = -\nabla h' + \mathbf{u} \times \boldsymbol{\omega} + \mathbf{g}$$

with $h' = h + \dot{\phi} = p + U + \frac{1}{2}|\mathbf{u}|^2 + \dot{\phi}$. This result may be integrated along any path C in the fluid from point P_1 to P_2 , yielding

$$h'(P_2) - h'(P_1) + \int_{P_1}^{P_2} \dot{\mathbf{u}}_\omega \cdot d\mathbf{x} = \int_{P_1}^{P_2} (\mathbf{u} \times \boldsymbol{\omega} + \mathbf{g}) \cdot d\mathbf{x}. \quad (38)$$

This result is already close to the desired relation. For example, if one Reynolds-averages with respect to a stationary ensemble, then $\overline{\dot{\mathbf{u}}_\omega} = \mathbf{0}$ and thus (38) reduces to Anderson's relation (28), in a slightly generalized form.

The key observation of Huggins is that another kind of average, a "mass-flux average," also makes the time-derivative term vanish. To explain this average, we must say a few words about "intrinsic" or "natural" coordinates for the incompressible potential flow \mathbf{u}_ϕ . This system takes as coordinate surfaces the iso-potential surfaces S_ϕ and the streamlines of \mathbf{u}_ϕ . As a coordinate variable along streamlines one may take ϕ itself or alternatively arclength ℓ , related by $d\phi = u_\phi d\ell$. The line-vector element along streamlines is thus $d\ell = \hat{\mathbf{u}}_\phi d\ell$. On a selected iso-potential surface S_ϕ one may introduce curvilinear coordinates ψ, χ to label the individual streamlines, completing the set (ϕ, ψ, χ) of natural/intrinsic coordinates. The area element on S_ϕ is given by $dA = |\frac{\partial \mathbf{x}}{\partial \psi} \times \frac{\partial \mathbf{x}}{\partial \chi}| d\psi d\chi$, in terms of which another positive measure may be defined as $dJ = \rho u_\phi dA$. This measure represents the mass-flux carried by the potential flow \mathbf{u}_ϕ across each subset of the surface S_ϕ . Note that it does not matter in the definition of dJ which iso-potential surface is considered, since dJ is constant along streamlines by incompressibility. For a general surface transverse to the potential flow, not necessarily an equi-potential surface, $dJ = \rho |\mathbf{u}_\phi \cdot \hat{\mathbf{n}}| dA$. The entire construction simplifies in two space dimensions. In 2D intrinsic orthogonal coordinates are (ϕ, ψ) , where ψ is the streamfunction which is the harmonic conjugate to the potential ϕ . In that case $dJ = \rho d\psi$.

The derivation is now easily completed. Take the integral in (38) along the streamlines crossing from surface S_{in} to surface S_{out} , and average with respect to dJ . It then follows from the b.c. (37) that the mass-flux of the potential flow is equal to the mass-flux of the full flow. The key term to analyze is $\int dJ \int \dot{\mathbf{u}}_\omega \cdot d\boldsymbol{\ell}$. Using $\varrho \mathbf{u}_\phi d^3x = \varrho u_\phi dA \cdot \hat{\mathbf{u}}_\phi d\boldsymbol{\ell} = dJ d\boldsymbol{\ell}$, this may be rewritten as

$$\int dJ \int \dot{\mathbf{u}}_\omega \cdot d\boldsymbol{\ell} = \varrho \int \dot{\mathbf{u}}_\omega \cdot \mathbf{u}_\phi d^3x = 0.$$

The latter integral vanishes by the same reasoning used to prove orthogonality of \mathbf{u}_ϕ and \mathbf{u}_ω . We finally obtain the *detailed Josephson relation* of [11]:

$$\int dJ h'_{in} - \int dJ h'_{out} = - \int dJ \int (\mathbf{u} \times \boldsymbol{\omega} + \mathbf{g}) \cdot d\boldsymbol{\ell} \quad (39)$$

The line-integrals on the righthand side are taken along streamlines of the potential flow and represent the generation of circulation along those lines. Substituting the decomposition (35) for \mathbf{g} one can see that there are two essential contributions, one from the line-integral of $\mathbf{u}_v \times \boldsymbol{\omega}$ which represents the transverse motion of vorticity across streamlines at velocity $\mathbf{u}_v = \mathbf{u} + \Delta \mathbf{u}$ and the other from the line-integral of $\alpha \boldsymbol{\omega}$ which represents acceleration by longitudinal forces. Note that one may also write

$$\int (\mathbf{u} \times \boldsymbol{\omega} + \mathbf{g}) \cdot d\boldsymbol{\ell} = \frac{1}{2} \int \epsilon_{ijk} \Sigma_{ij} d\ell_k,$$

in terms of the vorticity flux tensor (3). The lefthand side of (39) may be rewritten as

$$\int dJ h'_{in} - \int dJ h'_{out} = J [\langle h'_{in} \rangle_J - \langle h'_{out} \rangle_J],$$

where J is the total mass flux and $\langle \cdot \rangle_J = (1/J) \int (\cdot) dJ$ defines the mass-flux average. The energy relations (31)-(33) may be similarly generalized, with $J(h_{in} - h_{out})$ in (31) and (32) replaced with $J[\langle h_{in} \rangle_J - \langle h_{out} \rangle_J]$, and the transfer term $\kappa \dot{J}_\phi$ in (32) and (33) replaced with the righthand side of (39). For details of the proofs, see [11].

References

- [1] H. Tennekes and J. L. Lumley, *A First Course in Turbulence*. (MIT Press, Cambridge, MA, 1972).
- [2] H. Helmholtz, “Über Integrale der hydrodynamischen Gleichungen welche den Wirbelbewegungen entsprechen,” *Crelles Journal* **55** 25–55 (1858).
- [3] L. Föppl, “Wirbelbewegung hinter einem kreiszylinder. Sitzb. d. k. baeyr. Akad. d. Wiss.,” *Math-Physi. Klasse, München* **1** 1–17 (1913)
- [4] G. I. Taylor, “The transport of vorticity and heat through fluids in turbulent motion,” *Proc. Roy. Soc. Lond. A* **135** 685–705 (1932).
- [5] J.C. Klewicki, “Velocity-vorticity correlations related to the gradients of the Reynolds stresses in parallel turbulent wall flows,” *Phys. Fluids A* **1** 1285–1288 (1989)
- [6] J. C. Klewicki, J. Murray and R. E. Falco, “Vortical motion contributions to stress transport in turbulent boundary layers,” *Phys. Fluids* **6** 277–286 (1994).
- [7] P. J. A. Priyadarshana, J. C. Klewicki, S. Treat and J. F. Foss, “Statistical structure of turbulent-boundary layer velocity-vorticity products at high and low Reynolds numbers,” *J. Fluid Mech.* **570** 307–346 (2007).
- [8] J. Klewicki, P. Fife, T. Wei, and P. McMurty, “A physical model of the turbulent boundary layer consonant with mean momentum balance structure,” *Phil. Trans. R. Soc. A* **365** 823–839 (2007).
- [9] P. S. Bernard, “Turbulent vorticity transport in three dimensions,” *Theoret. Comput. Fluid Dyn.* **2** 165–183 (1990).
- [10] P. W. Anderson, “Considerations on the flow of superfluid helium,” *Rev. Mod. Phys.* **38** 298–310 (1966).

- [11] E. R. Huggins, “Energy dissipation theorem and detailed Josephson equation for ideal incompressible fluids,” *Phys. Rev. A* **1** 332–337 (1970).
- [12] W. Zimmerman, Jr., “Energy transfer and phase slip by quantum vortex motion in superfluid ^4He ,” *J. Low Temp. Phys.* **93** 1003–1018 (1993).
- [13] R. E. Packard, “The role of the Josephson-Anderson equation in superfluid helium,” *Rev. Mod. Phys.* **70** 641–651 (1998).
- [14] E. R. Huggins, “Vortex currents in turbulent superfluid and classical fluid channel flow, the Magnus effect, and Goldstone boson fields,” *J. Low Temp. Phys.* **96** 317–346 (1994).
- [15] F. A. Lyman, “Vorticity production at a solid boundary,” *Appl. Mech. Rev.* **43** 157–158 (1990)
- [16] Except possibly at isolated points where $\boldsymbol{\sigma} = \mathbf{0}$, in which case a normal component is permitted.
- [17] J. Z. Wu and J. M. Wu, “Vorticity dynamics on boundaries,” *Adv. in Appl. Mech.* **32** 119–275 (1996)
- [18] The pressure conditions, $\hat{\mathbf{n}} \times \nabla p = -\hat{\mathbf{n}} \times (D_t \mathbf{u} + \nu \nabla \times \boldsymbol{\omega} - \mathbf{f})$, which arises from the tangential components of the equation of motion at the boundary, are not automatically satisfied in Leray’s existence proof of Navier-Stokes solutions, which instead enforces the Neumann condition $\hat{\mathbf{n}} \cdot \nabla p = -\hat{\mathbf{n}} \cdot (D_t \mathbf{u} + \nu \nabla \times \boldsymbol{\omega} - \mathbf{f})$. However, Temam [19, 20] has proved that the tangential components of the equation of motion at the boundary emerge as necessary and sufficient “compatibility conditions” for a solution to remain smooth up to the wall.
- [19] R. Temam, “Behavior at time $t = 0$ of the solutions of semi-linear evolution equations,” *J. Diff. Eq.* **43** 73–92 (1982)
- [20] R. Temam, “Suitable initial conditions,” *J. Comp. Phys.* **218** 443–450 (2006)

- [21] C. H. Crawford and G. E. Karniadakis, “Reynolds stress analysis of EMHD-controlled wall turbulence. Part I. Streamwise forcing,” *Phys. Fluids* **9** 788–806 (1997)
- [22] Y. Dubief, V. E. Terrapon, C. M. White, E. S. G. Shaqfeh, P. Moin, and S. K. Lele, “New answers on the interaction between polymers and vortices in turbulent flows,” *Flow Turbul. Combust.* **74** 311–329 (2005).
- [23] K. Kim, R. J. Adrian, S. Balachandar and R. Sureshkumar, “Dynamics of hairpin vortices and polymer-induced turbulent drag reduction,” *Phys. Rev. Lett.* **100** 134504 (2008)
- [24] M. J. Lighthill, “Introduction: Boundary Layer Theory” in: *Laminar Boundary Theory* , L. Rosenhead, ed. (Oxford University Press, Oxford, 1963), pp.46–113.
- [25] B. R. Morton, “The generation and decay of vorticity,” *Geophys. Astrophys. Fluid Dyn.* **28** 277–308 (1984)
- [26] R. L. Panton, “Review of wall turbulence as described by composite expansions,” *Appl. Mech. Rev.* **58** 1–36 (2005)
- [27] T. Wei, P. Fife, J. Klewicki and P. McMurty, “Properties of the mean momentum balance in turbulent boundary layer, pipe and channel flows,” *J. Fluid Mech.* **522** 303–327 (2005).
- [28] P. Fife, J. Klewicki, P. McMurty and T. Wei, “Multiscaling in the presence of indeterminacy: wall-induced turbulence,” *Multiscale Model. Simul.* **4** 936–959 (2005).
- [29] R. R. Long and T.-C. Chen, “Experimental evidence for the existence of the mesolayer in turbulent systems,” *J. Fluid Mech.* **105** 19–59 (1981).
- [30] K. R. Sreenivasan, “A unified view of the origin and morphology of the turbulent boundary layer structure,” In: *Turbulence Management and Relaminarisation*, eds. H. W. Liepmann and R. Narasimha, (Springer-Verlag, 1987), pp. 37–61.

- [31] K. R. Sreenivasan and A. Sahay, “The persistence of viscous effects in the overlap region, and the mean velocity in turbulent pipe and channel flows,” In: *Self-Sustaining Mechanisms of Wall Turbulence*, ed. R. Panton (Computational Mechanics Publications, Southampton, UK, 1997), pp. 253–272.
- [32] B. Dubrulle, J. P. Lavalley, S. Nazarenko, and N. K.-R. Kevlahan, “A dynamic subfilter-scale model for plane parallel flows,” *Phys. Fluids* **13** 2045–2064 (2001).
- [33] T. Theodorsen, “Mechanism of turbulence,” In: *Proc. 2nd Midwestern Conf. of Fluid Mechanics*. (Ohio State University Press, Columbus, Ohio, 1952), pp.1–19.
- [34] M. R. Head and P. Bandyopadhyay, “New aspects of turbulent structure,” *J. Fluid Mech.* **107** 297–338 (1981)
- [35] P. Moin and J. Kim, “The structure of the vorticity field in turbulent channel flow. Part 1. Analysis of instantaneous fields and statistical correlations,” *J. Fluid Mech.* **155** 441–464 (1985).
- [36] J. Kim and P. Moin, “The structure of the vorticity field in turbulent channel flow. Part 2. Study of ensemble-averaged fields,” *J. Fluid Mech.* **162** 339–363 (1986).
- [37] H. E. Fiedler, “Coherent structures in turbulent flows,” *Prog. Aero. Sci.* **25** 231–270 (1988).
- [38] S. K. Robinson, “Coherent motions in turbulent boundary layers,” *Annu. Rev. Fluid Mech.* **23** 601–639 (1991).
- [39] R. J. Adrian, “Hairpin vortex organization in wall turbulence,” *Phys. Fluids.* **19** 041301 (2007).
- [40] A. E. Perry and M. S. Chong, “On the mechanism of wall turbulence,” *J. Fluid Mech.* **119** 173–217 (1982).
- [41] A. E. Perry, S. Henbest, and M. S. Chong, “A theoretical and experimental study of wall turbulence,” *J. Fluid Mech.* **165** 163–199 (1986).

- [42] A. E. Perry and I. Marusic, “A wall-wake model for the turbulence structure of boundary layers. Part 1. Extension of the attached eddy hypothesis,” *J. Fluid Mech.* **298** 361–388 (1995).
- [43] I. Marusic, “On the role of large-scale structures in wall turbulence,” *Phys. Fluids* **13** 735–743 (2001)
- [44] T. B. Nickels, I. Marusic, S. Hafez, N. Hutchins, and M.S. Chong, “Some predictions of the attached eddy model for a high Reynolds number boundary layer,” *Phil. Trans. R. Soc. A* **365** 807–822 (2007).
- [45] A. A. Townsend, *The Structure of Turbulent Shear Flow*, 2nd Ed. (Cambridge University Press, Cambridge, 1976).
- [46] R. J. Adrian, S. Balachandar, and Z.-C. Liu, “Spanwise growth of vortex structure in wall turbulence,” *KSME Int. J.* **15** 1741–1749 (2001)
- [47] C. D. Tomkins and R. J. Adrian, “Spanwise structure and scale growth in turbulent boundary layers,” *J. Fluid Mech.* **490** 37–74 (2003)
- [48] M. Tinkham, *Introduction to Superconductivity*, 2nd edition. (McGraw-Hill, New York, 1996)
- [49] J. F. Annett, *Superconductivity, Superfluids and Condensates*. (Oxford University Press, Oxford, 2004)
- [50] L. Onsager, Discussion remark on C. J. Gorter, “The two fluid model for Helium II,” International Conference on Statistical Mechanics, Florence, 1949. *Nuovo. Cim. Suppl.* **6** 249–250 (1949)
- [51] R. P. Feynman, “Application of quantum mechanics to liquid helium,” in: *Progress in Low Temperature Physics*, Vol.1. ed. C. Gorter (North-Holland, Amsterdam, 1955). pp. 17–51.

- [52] F. London, “On the problem of the molecular theory of superconductivity,” *Phys. Rev.* **74** 562–573 (1948).
- [53] A. A. Abrikosov, “An influence of the size on the critical field for type II superconductors,” *Dokl. Akad. Nauk SSSR* **86** 489–492 (1952)
- [54] A.A. Abrikosov, “Magnetic properties of superconductors of the second group,” *Zh. Eksp. Teor. Fiz.* **32** 1442–1452 (1957) [*Sov. Phys. JETP* **5** 1174–1182 (1957)].
- [55] P. W. Anderson, “Theory of flux creep in hard superconductors,” *Phys. Rev. Lett.* **9** 309–311 (1962)
- [56] B. D. Josephson, “Potential differences in the mixed state of type-II superconductors,” *Phys. Lett.* **16** 242–243 (1965)
- [57] W. Thomson (Lord Kelvin), “Notes on hydrodynamics: On the vis-viva of a liquid in motion,” *Camb. Dubl. Math. J.* **4** (1849)= *Mathematical & Physical Papers*, vol. 1, 107–112.
- [58] D. Thouless, P. Ao, Q. Niu, M. Geller, and C. Wexler, “Quantized vortices in superfluids and superconductors,” *Int. J. Mod. Phys. B* **13** 675–686 (1999).
- [59] P. Ao and X.-M. Zhu, “Microscopic theory of vortex dynamics in homogeneous superconductors,” *Phys. Rev. B* **60** 6850–6877 (1999)
- [60] A. Brissaud, U. Frisch, J. Leorat, M. Lesieur and A. Mazure, “Helicity cascades in fully developed isotropic turbulence,” *Phys. Fluids* **16** 1366–1367 (1973).
- [61] U. Frisch, Z. S. She and P. L. Sulem, “Large-scale flow driven by the anisotropic kinetic alpha effect,” *Physica D* **28** 382–392 (1987).
- [62] M. Guala, B. Lüthi, A. Liberzon, A. Tsinober, and W. Kinzelbach, “On the evolution of material lines and vorticity in homogeneous turbulence,” *J. Fluid Mech.* **533** 339–359 (2005).

- [63] G. L. Eyink, “Cascade of circulations in fluid turbulence,” *Phys. Rev. E* **74** 066302 (2006).
- [64] S. Chen, G. L. Eyink, M. Wan and Z. Xiao, “Is the Kelvin theorem valid for high Reynolds number turbulence?” *Phys. Rev. Lett.* **97** 144505 (2006).
- [65] G. Blatter, M. V. Feigel’man, V. B. Geshkenbein, A. I. Larkin, and V. M. Vinokur, “Vortices in high-temperature superconductors,” *Rev. Mod. Phys.* **66** 1125–1388 (1994)
- [66] D. P. Norton, “Science and technology of high-temperature superconducting films,” *Annu. Rev. Mater. Sci.* **28** 299–343 (1998).
- [67] A Gurevich, “Pinning size effects in critical currents of superconducting films,” *Supercond. Sci. Technol.* **20** S128–S135 (2007).
- [68] D. J. Bishop, P. L. Gammel and D. A. Huse, “Resistance in high-temperature superconductors,” *Scientific American*, February 1993, 48–55.
- [69] A. Matsumoto, H. Kumakura, H. Kitaguchi, B. J. Senkowicz, M. C. Jewell, E. E. Hellstrom, Y. Zhu, P. M. Voyles, and D. C. Larbalestier, “Evaluation of connectivity, flux pinning, and upper critical field contributions to the critical current density of bulk pure and SiC-alloyed MgB₂,” *Applied Phys. Lett.* **89** 132508 (2006)
- [70] B. J. Senkowicz, R. J. Mungall, Y. Zhu, J. Jiang, P. M. Voyles, E. E. Hellstrom, and D. C. Larbalestier, “Nanoscale grains, high irreversibility field and large critical current density as a function of high-energy ball milling time in C-doped magnesium diboride,” *Supercond. Sci. Technol.* **21** 035009 (2008).
- [71] C. J. Swanson, R. J. Donnelly, and G. G. Ihas, “Turbulent pipe flow of He I and He II,” *Physica B* **284–288** 77–78 (2000)
- [72] T. Xu and S. W. Van Sciver, “Particle image velocimetry measurements of the velocity profile in He II forced flow,” *Phys. Fluids* **19** 071703 (2007)

- [73] A.L. Yarin, “On the mechanism of turbulent drag reduction in dilute polymer solutions: dynamics of vortex filaments,” *J. Non-Newtonian Fluid Mech.* **69** 137–153 (1997).